Case Report

# Intraluminal Contrast-Enhanced Ultrasonography Application in Dogs and Cats

Saran Chhoey , Soyeon Kim , Eunjee Kim , Dongjae Lee , Kroesna Kang , Sath Keo , Jezie Alix Acord , Junghee Yoon , Jihye Choi [*]

*Case Report*

# Intraluminal contrast-enhanced ultrasonography application in dogs and cats

**Saran Chhoey [1,2], Soyeon Kim [3,4], Eunjee Kim [3], Dongjae Lee [3], Kroesna Kang [2], Sath Keo [2], Jezie A. Acorda [5], Junghee Yoon [3] and Jihye Choi [3,*]**

[1] Graduate School, Royal University of Agriculture, Phnom Penh, Cambodia; saranchhoey@rua.edu.kh

[2] Faculty of Veterinary Medicine, Royal University of Agriculture, Phnom Penh, Cambodia; kkroesna@rua.edu.kh; keosth@gmail.com

[3] Veterinary Medical Imaging, College of Veterinary Medicine, Seoul National University, Gwanak-ro 1, Gwanak-gu, Seoul 08826, South Korea; valerie_kim@naver.com; ej08ee@snu.ac.kr; yc4537@gmail.com; heeyoon@snu.ac.kr

[4] Department of Veterinary Medical Imaging, College of Veterinary Medicine, Chonnam National University, Yongbong-ro 77, Buk-gu, Gwangju 61186, South Korea.

[5] College of Veterinary Medicine, University of the Philippines Los Baños, Laguna 4031, Philippines; jaacorda@up.edu.ph

**\*** Correspondence: imsono@snu.ac.kr; Tel.: +82-2880-1278

**Simple Summary:** In this retrospective study, three dogs and three cats were selected from the da-tabases of the Chonnam National University Teaching Hospital from February 2017 to June 2019. The inclusion criteria for the selection of patients were as follows: (1) clinical data including age, sex, breed, clinical signs, histology, fine-needle aspiration, or fluid centesis were available, and (2) intraluminal CEUS was performed, and CEUS findings helped confirmed the diagnosis. Each patient underwent physical examination, blood tests, radiography, and conventional ultrasonography. Intraluminal CEUS was performed using contrast agents, including SonoVue, agitated saline, saline, or a combination for GI hydrosonography in two patients and sono-cystourethrography in four patients. GI hydrosonography could assess the anatomic relationship between the mass and gastric lumen after administration of a mixture of 0.1 mL SonoVue and 30 mL/kg water in case 1 and could dilate the colonic lumen to detect the thickened wall using saline infusion in case 2. On sono-cystourethrography, communication between the urinary tract and prostatic cyst was clearly visualized in case 3, and narrowing of the urethral lumen secondary to prostatomegaly could be ruled out in case 4 with pyogranulomatous prostitis using agitated saline. The saline or agitated saline is appropriate for filling the lumen and improving the acoustic window for GI hydrosonography. Intraluminal CEUS examinations helped to assess the patency of the lumen, evaluate the extent of luminal dilation, rule out luminal narrowing, determine the presence of a mass within the lumen, and identify rupture sites.

**Abstract:** Administering intraluminal fluid can improve the acoustic window for visualization of lumen and wall layers in the cavitary organs. Microbubbles in ultrasound contrast agents can also be used for intracavitary applications to enhance visualization of the lesion in human patients. However, there was no literature extending the clinical application of the intraluminal contrast-enhanced ultrasonography (CEUS) to patients with naturally occurring diseases in veterinary medicine. This case series aims to describe the detailed application and diagnostic value of intraluminal CEUS in six clinical cases with naturally occurring gastrointestinal (GI) and urinary tract diseases.

**Keywords:** canine; CEUS; feline; gastrointestinal; urinary

## 1. Introduction

Ultrasonography Ultrasonography provides real-time evaluation of abdominal organs regarding shape, echogenicity, echotexture, margin, blood flow, and motility in veterinary medicine [1,2,3]. However, despite its extensive use, ultrasonographic assessment encounters limitations, particularly in imaging gas-filled structures, in visualizing narrow-lumen structures, or identifying

sites of small organ rupture, attributed to suboptimal acoustic windows and limited spatial resolution [4].

To circumvent these challenges, administering intraluminal fluid can improve the acoustic window for visualization of lumen and wall layers and enabling precise measurement of the wall thickness in a fluid-dilated stomach, compared to an empty or collapsed stomach [5]. In human medicine, injecting fluid into the endometrial cavity assists in visualizing pathologic lesions, such as myomas, polyps, adhesions, and congenital anomalies, though it provides limited information on tubal patency [6]. Hydrosonography is a simple technique that can be easily performed in patients without the need for anesthesia. In GI hydrosonography, ultrasonography uses fluid to distend the GI tract by fluid administration and improve the acoustic window to evaluate the gastric wall and lumen.

Ultrasound contrast agents (UCAs) consist of gas-filled microbubbles encapsulated in a shell that resonate when displayed on an ultrasound beam, enhancing imaging [7,8]. Contrast enhanced ultrasonography (CEUS) generally evaluates the perfusion of lesions after intravenous injection of UCAs [9,10,11,12,13,14,15,16,17,18]. CEUS allows real-time evaluation of wash-in and wash-out of the contrast agent and provides hemodynamic information representative of the blood volume and flow rate in the lesion. Because microbubbles can generate hyperechoic signals by reflecting and scattering sound waves, UCAs can also be used for intracavitary applications, as an intraluminal CEUS, to enhance visualization of abscesses or fistulas in human patients [19,20,21,22]. For instance, the sulfur-hexafluoride, SonoVue® (Braco, Milan, Italy), has used to guide abscess drainage by being injected via drainage catheters. while hydrogen peroxide has helped identify anal fistulas and their internal openings by injection into the fistula tract [23,24,25,26,27,28].

Despite its proven benefits in human medicine, there have been only four reports of intraluminal CEUS use in veterinary medicine [28,29,30,31,32]. Traditionally, 30 mL/kg of tap water has been used for GI hydrosonography. In a previous study, GI hydrosonography using SonoVue for the assessment of the GI tract was evaluated by comparing non-contrast ultrasonography and hydrosonography using water in healthy beagle dogs [28]. After intraluminal administration of 0.1 mL of SonoVue mixed with 30 mL/kg of water into the stomach, wall thickness, wall layer definition, conspicuity of the mucosal surface, and image quality were evaluated in the gastric cardia, body, pylorus, and descending duodenum [29]. GI hydrosonography using SonoVue significantly improved the wall definition and mucosal conspicuity in the near fields of the gastric body, pylorus, and duodenum compared to the non-contrast method and the pylorus compared to the water method [29,33].

Sono-urethrography, another application, assesses urethral integrity through fluid dilation of the urethral lumen. In a previous study, sono-urethrography using saline, agitated saline, and SonoVue was performed to evaluate urethral integrity by fluid dilation of the urethral lumen and urethral wall thickening in male dogs [28] and human [34]. In sono-urethrography, saline, and agitated saline are recommended for evaluation of the urethral wall and lumen, and an UCA for evaluation of the integrity of the urethra by improving its conspicuity. In another study, contrast-enhanced voiding ultrasonography was performed after injecting a gently shaken mixture of 1 mL of SonoVue and 250 mL of 0.9% saline through a urinary catheter into the urinary bladder and urethra in healthy dogs [31]. Contrast-enhanced cystosonography using 1 mL/kg agitated saline, predetermined to contain 20% air by volume, was used to detect urinary bladder ruptures in 17 dog cadavers [32].

The majority of these studies assessed the feasibility of intraluminal CEUS in healthy dogs however there was no literature extending its clinical application to patients with naturally occurring diseases. Therefore, in this study, the intraluminal CEUS features were described in dogs and cats that underwent intraluminal CEUS examinations of the GI tract and lower urinary tract. This study aimed to introduce the clinical application of intraluminal CEUS in dogs and cats.

## 2. Case Description

This case series included three dogs and three cats that underwent intraluminal CEUS using various contrast agents, including SonoVue, agitated saline, and saline, or a combination thereof. Two patients received GI hydrosonography, and four patients underwent sono-cystourethrography. All intraluminal CEUS examinations were conducted using an ultrasound machine (Prosound Alpha 7, Hitachi-Aloka, Tokyo, Japan) with a 10 MHz linear transducer by a radiologist (J.H.C.). The time gain control was set at its central position and the power was set at a constant level, with a gain of 64 dB.

### 2.1. Case 1

A 12-year-old spayed female Maltese presented with vomiting, anorexia and polydipsia for two weeks. The patient showed mild anemia, increased blood urea nitrogen (>130 mg/dL, reference range; 7–27 mg/dL) and creatinine (>2.7 mg/dL, reference range; 0.5–1.8 mg/dL) levels, hyperphosphatemia (14.6 mg/dL, reference range; 2.5–6.8 mg/dL) and hypokalemia (2.5 mmol/L, reference range; 3.5–5.8 mmol/L). Urine specific gravity was 1.014. Ultrasonography revealed hyperechoic change of bilateral renal cortex with attenuation of corticomedullary definition, leading to a diagnosis of chronic renal disease. A crater-like mucosal defect filled with hyperechoic gas was identified in the gastric wall at the pylorus (Figure 1). The adjacent gastric wall appeared uniformly thickened with an irregular mucosal surface and poorly defined wall layers. Additionally, a focal hypoechoic thickened lesion measuring 9.6 mm in thickness was observed. Due to the stomach being mostly contracted and filled with a significant amount of gas, it was difficult to accurately assess the thickness of the gastric wall and the extent of the lesion, and it was challenging to determine whether the layers of the stomach wall were lost. Therefore, GI hydrosonography was conducted with the oral administration of 100 ml of saline. The saline expanded the stomach and reduced the degradation of the quality of the ultrasound images caused by gas effects. The mucosal defect was measured 16.9 mm in length and located in the gastric body. Gas accumulation within the gastric wall appeared as an echogenic line. In the dilated pylorus, another crater-like lesion was clearly visible, which was thinner wall thickness (2.6 mm) compared to the adjacent normal layer thickness (5.9 mm). The focal thickened area of the pyloric wall was measured at 25 x 6.7 mm, with a loss of clear definition in the wall layers. The gastric wall thickening was considered as uremic gastropathy induced by chronic renal failure. The azotemia was alleviated over 14 days with medication however the dog was euthanized due to the grave prognosis of chronic renal failure. The gastric lesion was determined as moderate multifocal erosion histopathologically.
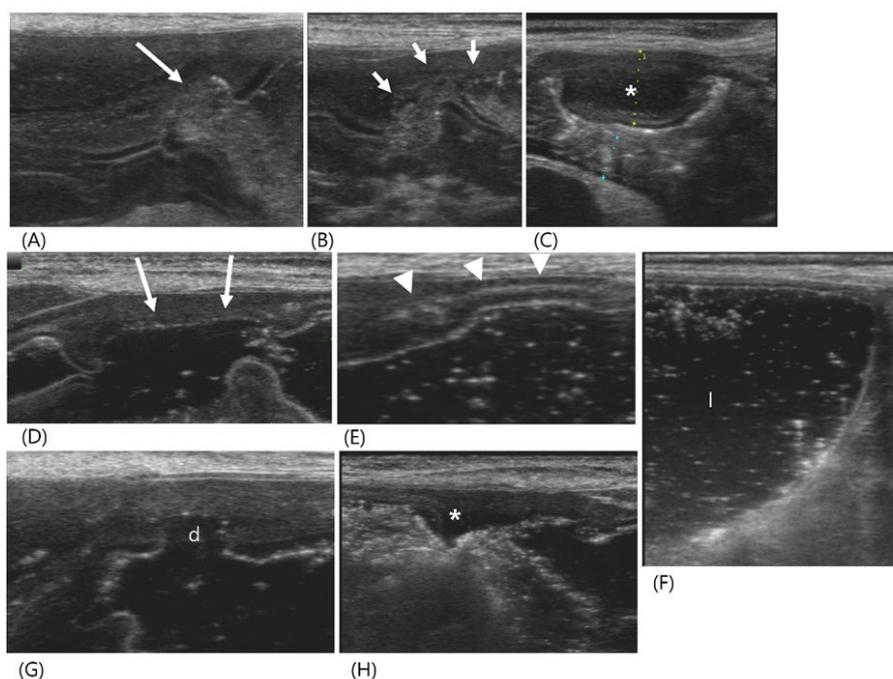


(A)    (B)    (C)
(D)    (E)    (F)
(G)    (H)

**Figure 1.** Ultrasonography of a 12-year-old spayed female maltese (Case 1) with uremic gastropathy before **(A-C)** and after GI hydrosonography **(D-H)**. On conventional ultrasonography, **(A)** a crater-like mucosal defect (long arrow) was filled with hyperechoic gas in the gastric wall at the pylorus. **(B)** The collapsed pyloric antrum (short arrows) had uniformly thickened wall with an irregular mucosal surface and poorly defined layers. **(C)** A focal hypoechoic wall thickening (asterisk) was shown. **(D-H)** After oral administration of saline, the gastric lumen was filled with fluid. **(D)** The mucosal defect (long arrows) was larger than that in **(A)** and located in the gastric body but not in the pylorus. **(E)** Note the echogenic line (arrowheads) within the gastric wall generated by intramural gas accumulation. **(F)** Normal wall thickness and layers were detected by the dilated gastric lumen (l). **(G, H)** The pylorus had irregular wall thickness due to another crater-like lesion (d) clearly thinner compared to the adjacent wall and focal thickened area (asterisk). Note a loss of clear definition in the wall layers in the focal thickened area.

### 2.2. Case 2

A 6-month-old Scottish Fold cat, diagnosed with feline infectious peritonitis, presented with intermittent vomiting, diarrhea, and constipation over the course of a week. Conventional ultrasonography revealed a small amount of anechoic fluid, generalized swollen abdominal fat, moderately enlarged lymph nodes, and hyperechoic renal cortex with medullary rim sign in both kidneys. The wall thickness and layers of the ascending and transverse colons appeared normal (Figure 2). However, the descending colon showed marked wall thickening, measuring 10 mm in thickness over a length of approximately 70 mm, and fecal retention was observed immediately proximal to the thickened area of the colon. In particular, the thickening of the muscular layer was considered however luminal obstruction and definition of wall layers could not be confirmed because the colon was collapsed, which could make the wall appear thick. GI hydrosonography was performed by administering 10 mg of tap water via a rectal catheter to assess the extent of thickened descending colon and evaluate the colonic wall. The distal part of the descending colon which appeared thickened and corrugated in conventional ultrasonography was dilated normally and showed a regular mucosal surface and thin walls. However, the proximal two-thirds of the descending colon was not show expansion of the lumen due to hypertrophied bowel walls, and all layers of the bowel wall appeared to be preserved normally. However, the muscular layer was markedly hypertrophied, suggesting inflammatory changes related with feline infectious peritonitis. Compared to conventional ultrasonography, the use of a GI hydrosonography provided clearer assessment of the length of the hypertrophied bowel walls and evaluation of the wall layers.
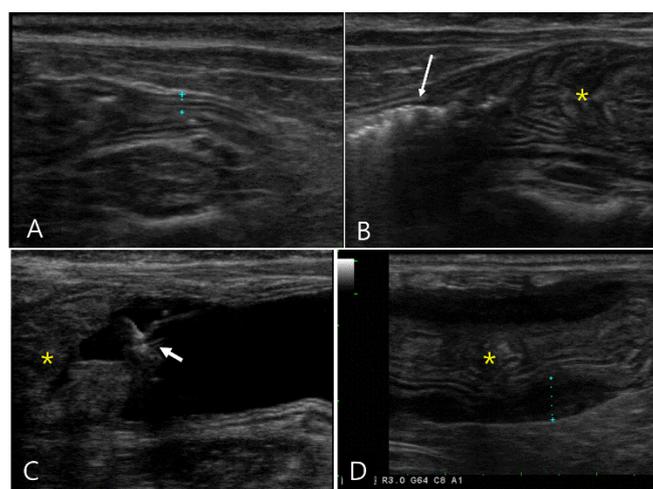


**Figure 2.** Longitudinal images of abdominal ultrasonography in a 6-month-old Scottish fold cat diagnosed with feline infectious peritonitis (Case 2) pre- **(A, B)** and post-GI hydrosonography **(C, D).** On conventional ultrasonography, **(A)** the ascending colon (arrowhead) had a normal wall thickness (1.96 mm) with distinct layer delineation. **(B)** The descending colon (asterisk) exhibits marked thickening, measuring 1 cm in thickness and extending over 7 cm in length, with collapsed lumen.

Note the presence of gas and feces (long arrow) proximal to affected area. **(C)** Following saline infusion via a rectal catheter (short arrow), the distal descending colon was normally dilated with anechoic fluid (f) visible. **(D)** The proximal two-thirds of the descending colon (*) showed no lumen expansion; the muscular layer (m) was markedly hypertrophied, although the wall layers remain normally preserved.

### 2.3. Case 3

An 11-year-old intact male Pekingese presenting with dark brown or bloody hematuria and decreased appetite for 15 days. Physical and laboratory examinations were within normal ranges, including serum creatinine (0.9 mg/dL; reference range 0.5–1.8 mg/dL) and blood urea nitrogen (18 mg/dL; reference range 7 – 27 mg/dL) levels. Conventional ultrasonography revealed an asymmetrically enlarged prostate. The right lobe was replaced by a cystic lesion (46.27 x 31.86 mm) containing hyperechoic fluid with loss of most of the prostatic parenchyma (Figure 3). The prostatic urethra was dilated and displaced to the left by the enlarged right prostate lobe. The urinary bladder and urethra contained hyperechoic sludge, and the bladder wall was thickened. The peri-prostatic fat was normal; however, the medial iliac lymph nodes were enlarged to approximately 12 mm, with an oval shape. Because the hypoechoic fluid mixed with hyperechoic materials, suggestive of infected sludge was found in the urinary bladder and prostatic cyst, communication between the urinary tract and the prostatic cyst was suspected but not be confirmed using conventional ultrasonography. Therefore, sono-urethrography was performed by injecting agitated saline into the urethra via a 6-French urinary catheter that was passed into the distal penile urethra. After connecting two syringes, one containing 20 ml of 0.9% saline and the other empty, to a three-way stopcock, agitated saline was prepared by the rapid injection of saline from the full syringe into the empty syringe several times. Then, the agitated saline was immediately injected into the urethral catheter. The hyperechoic bubbles flowed into the urinary bladder, and some of them leaked into the prostatic cyst. Communication between the urinary bladder and the prostatic cyst was clearly observed because the saline bubbles showed hyperechoic signals in contrast to the hypoechoic fluid in the cyst. Under ultrasound guidance, approximately 20 ml of turbid, creamy, yellow fluid was obtained from the prostatic cyst using a 23-gauge catheter. The sampled fluid was analyzed: total nuclear cell count was 55.33 K/$\mu\ell$, specific gravity was 1.020, creatinine level was 48.8 mg/dL, fluid/serum creatinine ratio was 54.2, and total protein level was less than 2.0 g/dL. The fluid contained degenerated neutrophils and rod-shaped bacteria. Streptococcus and Pasteurella were detected in both fluid and urine cultures. Benign prostatic hyperplasia, prostatic urethral leakage, a prostatic cyst, and subsequent lower urinary tract infection were confirmed. Castration was performed, and antibiotics were administered.
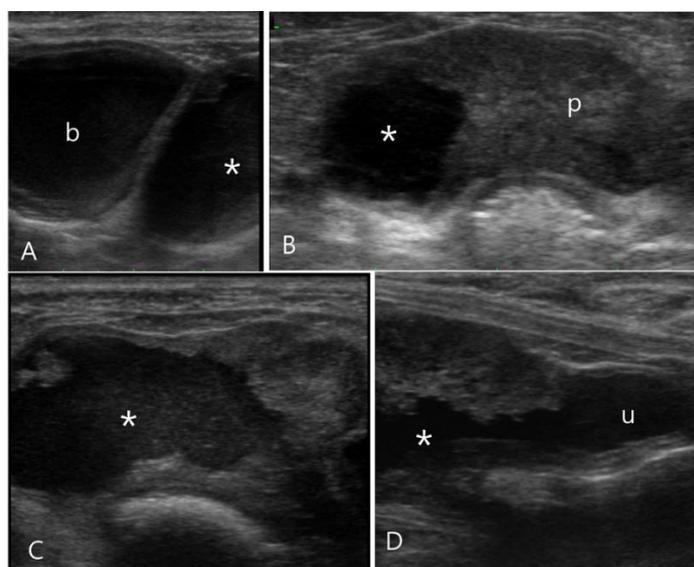
6

**Figure 3.** Ultrasonography of the prostatic cyst in a 11-year-old intact male Pekingese (Case 3). **(A)** On longitudinal ultrasound image, the asymmetrically enlarged prostate with a cystic formation (asterisk) was observed caudal to the bladder (b). **(B)** Transverse ultrasound image revealed the right prostate lobe almost entirely replaced by a cystic lesion filled with hyperechoic fluid. **(C, D)** Sono-urethrography images obtained using agitated saline to enhance contrast, displaying the presence of microbubbles indicating the echogenic fluid leakage into the prostatic cyst. Additionally, these images demonstrate a clear communication between the prostatic cyst and urethra (u).

*2.4. Case 4*

A 12-year-old intact male Shih Tzu was presented with symptoms of dysuria, anorexia, and depression. The dog was diagnosed with urethral calculi approximately 2 years before and recently experienced pain during urination. Clinical examination and findings on complete blood count and serum biochemistry evaluation were unremarkable. On conventional ultrasonography, a calculus, approximately 3.5 mm in diameter, was visible in the penile urethra; however, there was no dilation of the urethral lumen. The prostate was enlarged to approximately 20 × 23 mm and showed a mildly heterogeneous echotexture with hypoechoic areas (Figure 4). It had regular margins, and there was no cyst or mineralization within the prostatic parenchyma. The prostatic urethra was not clearly observed, and it was difficult to confirm patency or obstruction of the urethral lumen. The medial iliac lymph nodes were mildly enlarged to 1.4 cm in length, but their shapes were normal. The prostatomegaly was attributed to benign prostatic hyperplasia, with the likelihood of a prostatic tumor considered low, because the dog was a neutered male. To evaluate the prostate parenchyma, CEUS was performed after the intravenous injection of 0.125 ml/kg SonoVue, followed by a bolus of 5 ml saline through the cephalic vein. This examination was performed in the extended pure harmonic detection mode with the focus point set at the bottom for homogeneous energy distribution over the image. The transmitted energy was reduced to magnitudes of 7% and the MI used were 0.07. In the wash-in phase, both the prostatic lobes were simultaneously enhanced; however, the left lobe showed a faster washout than the right lobe. Sono-urethrography by injecting agitated saline via a 6-French urinary catheter that was passed into the distal penile urethra was performed to evaluate the narrowing of the urethral lumen secondary to prostatomegaly and to determine the cause of the dysuria. Microbubbles passing through the intact lumen of the prostatic urethra were clearly visible, and there was no evidence of abnormal changes in the urethral mucosa. Urethral compression or obstruction was ruled out. Fine-needle aspiration of the left prostatic lobe revealed pyogranulomatous inflammation of the prostatic parenchyma.
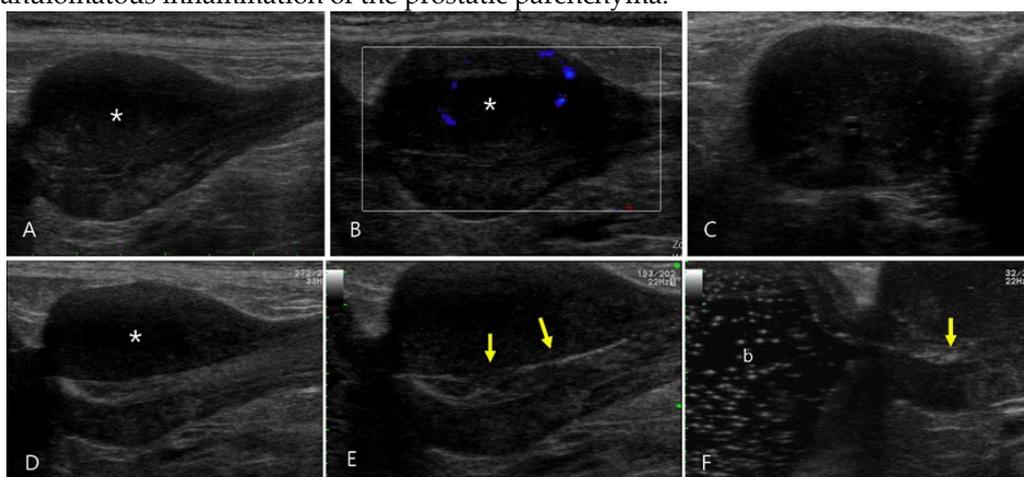


**Figure 4.** Ultrasonography of pyogranulomatous inflammation of the prostate in a 12-year-old intact male Shih Tzu (Case 4). **(A)** Prostatomegaly characterized by a regular margin and mildly heterogeneous echotexture, with notable hypoechoic changes in the parenchyma of the left lobe (asterisk) was observed. **(B)** Color flow Doppler images revealed minimal vascular signal in the prostate, suggesting low blood flow. **(C-E)** Sono-urethrography conducted with agitated saline showed microbubbles transiting through the intact lumen of the prostatic urethra, highlighting the

regular appearance of the urethral mucosal surface (arrows). **(F)** The echogenic bubbles flowed into the urinary bladder (b), confirming the absence of urethral compression or obstruction.

### 2.5. Case 5

A 3-year-old neutered male Russian Blue who developed acute ascites following cystocentesis performed for feline idiopathic cystitis at a local clinic. Laboratory tests revealed the elevation of the serum creatinine (3.7 mg/dL; reference range 0.8 – 2.4) and lipase (168 U/L; reference range 0 – 35 U/L) levels and mild hyponatremia (139.5 mmol/L; reference range 146 – 157 mmol/L) and hypochloremia (113.6 mmol/L; reference range 116–126 mmol/L). On conventional ultrasonography, a large amount of peritoneal fluid surrounded the urinary bladder. A hyperechoic line was observed within the bladder wall, which was suspected to be the ruptured area. Sonocystography was performed to determine the ruptured area (Figure 5). Initially, agitated saline was administered via a urethral catheter, and the bladder was distended normally without significant leakage of bubbles into the peritoneal cavity. Sono-cystography using SonoVue was conducted by injecting 0.5 ml (25 mg) of the UCA, followed by a 5 ml saline flush. The strong bright signal of the microbubbles indicated leakage from the suspected ruptured area of the bladder into the peritoneal space. The bladder rupture was treated by keeping a urinary catheter in place for approximately 3 days instead of performing a laparotomy because the ruptured area was very small. Sono-urethrography showed a small defect in the urinary bladder wall in the previously ruptured region; however, there was no evidence of bubble leakage.
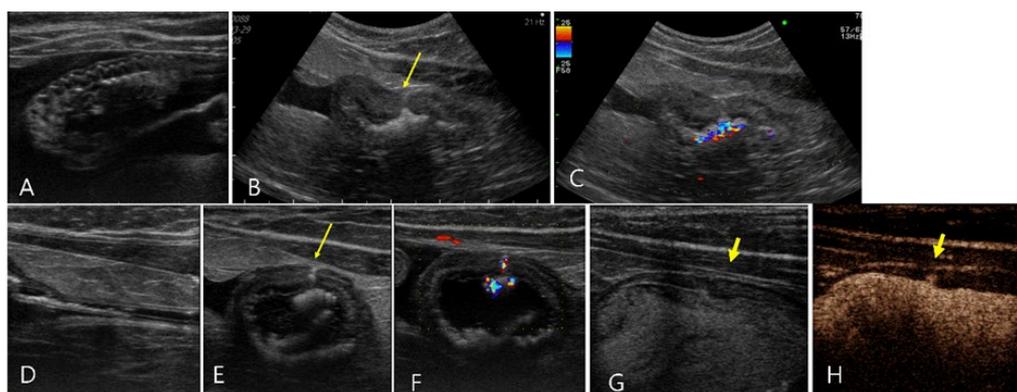


**Figure 5.** Ultrasonography of a 3-year-old neutered male Russian Blue (Case 5) presenting with urinary bladder rupture initially observed on day 1 **(A-F)** and subsequent findings 3 days post-catheterization **(G, H)**. **(A, B)** Initial conventional ultrasonography revealed a large amount of peritoneal fluid surrounding the urinary bladder and a hyperechoic line (long arrow) indicative of a tear on the ventral aspect of the bladder wall. There were echogenic contents with acoustic shadowing in the bladder. **(C)** Note color-Doppler signals emanating from these echogenic contents, suggestive of the presence of gas or calculi. **(D-F)** Sono-urethrography using SonoVue demonstrated the strong bright signal of microbubbles indicating an intact urethra, with notable leakage (long arrow) of these bubbles from the damaged bladder wall into the peritoneal cavity, confirming bladder rupture. **(F)** Note the color signal within the bladder wall, attributed to microbubble presence. Follow-up sono-urethrography conducted 3 days after bladder catheterization showed a small defect in the bladder wall but no evident microbubble leakage, either on conventional B-mode **(G)** or harmonic mode **(H)** imaging, suggesting partial healing of the bladder wall.

### 2.6. Case 6

A 2-year-old male mixed cat was presented with symptoms of depression and abdominal distension, suggestive of urinary bladder rupture following trauma. On conventional ultrasonography, the urinary bladder was empty and collapsed to a thickness of 8 mm at the bladder wall. Cystic lesions (28.6 x 20 mm) containing echogenic fluid were observed on the right side of the bladder apex. The cystic structures appeared to be located within the bladder wall without a clear

distinction from the remaining bladder. Large amounts of anechoic peritoneal effusion and hyperechoic swelling of fat were observed in the caudal abdomen. Approximately 470 ml of the effusion was removed via abdominal centesis. Sono-urethrography was additionally performed to demonstrate the anatomic relationship between the cystic structure and the urinary bladder and to evaluate their integrities (Figure 6). When agitated saline was used, echogenic bubbles filled the bladder; however, bladder rupture was not identified. However, when the sono-urethrography was repeated using SonoVue, the contrast agent flowed through the bladder and the cystic lesion. Echogenic linear leakage of the microbubbles was clearly observed from the cystic lesion, which flowed into the abdominal cavity. Laparotomy confirmed a bladder defect at the apex with a hematoma.
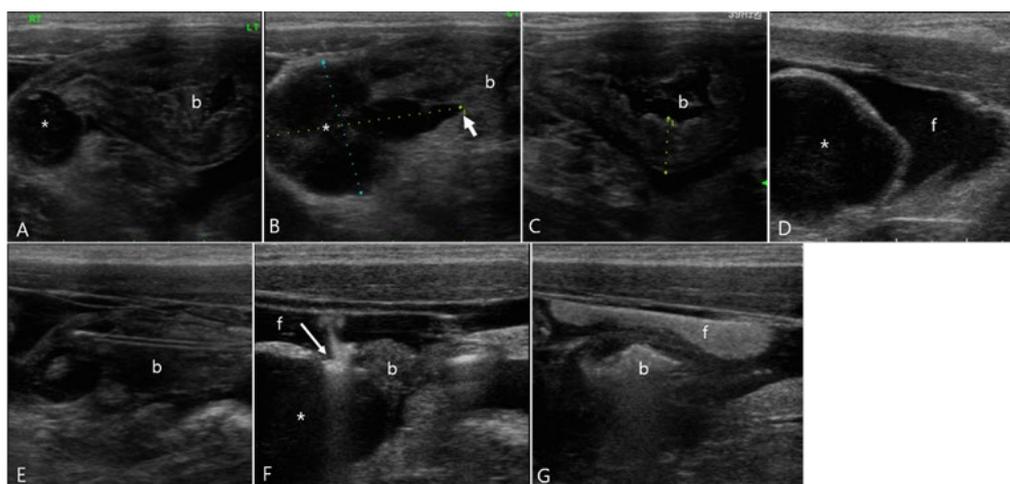


**Figure 6.** Ultrasonography of urinary bladder rupture in a 2-year-old male mixed cat (Case 6). **(A, B)** Cystic lesions (asterisk) filled with echogenic fluid were found within the bladder wall, located at the right side of the bladder apex. **(C)** The urinary bladder (b) was collapsed with an empty lumen and a bladder wall thickness of 8 mm. **(D)** Extensive anechoic peritoneal effusion (f) was surrounding the cystic lesion (asterisk). **(E-G)** On sono-urethrography using SonoVue, a distinct echogenic linear leakage of the microbubbles (long arrow) emanates from the cystic lesion, dispersed into the surrounding anechoic peritoneal effusion (f). **(E)** The urinary catheter was visualized as echogenic double lines in the bladder. **(G)** Note the change of echogenicity of the peritoneal effusion after sono-urethrography, indicating the diffusion of SonoVue microbubbles.

## 3. Discussion

This retrospective study introduced the clinical application of intraluminal CEUS for GI and urinary tracts in dogs and cats. Intraluminal CEUS in GI hydrosonography and sono-urethrography improved the visualization of lesions in naturally occurring diseases.

In the present study, GI hydrosonography was performed in the upper GI tract and colon. Traditionally, GI hydrosonography is performed using tap water [5, 29]. In human medicine, antifoaming agents such as simethicone and microsphere UCAs such as SonoVue are used for GI hydrosonography [5, 35, 36]. In the present study, a mixture of SonoVue and water was used as the contrast agent for GI hydrosonography of the stomach rather than using water only. A sufficient amount of anechoic water improved the acoustic window by filling the stomach, and hyperechoic microbubbles clearly enabled visualization of the lumen extending from the gastric fundus to the pylorus by enhancing the mucosa-lumen interface. This result is comparable to those of previous studies performed in healthy dogs and human patients [5, 29, 35]. GI hydrosonography using a SonoVue and water mixture in healthy dogs showed the homogeneous echogenicity of the luminal border and improved wall layer definition and mucosal conspicuity of the GI tract compared with non-contrast studies or GI hydrosonography using water only in healthy dogs [29]. The dilution ratio of UCA to water may affect the image quality. In human studies, approximately 0.05 to 0.1 mL of SonoVue was mixed with 200 mL of tap water. However, the present study was conducted using the

same dilution ratio and volume of the UCA used in a previous healthy canine study since the study provided image quality good enough to evaluate the wall and lumen of the GI tract [29].

In case 2, we used only water for hydrosonography of the colon to differentiate true wall thickening from pseudo-thickening caused by collapse of an empty colon. Colonic wall thickness can be affected by luminal contents [37]. When the colon was evaluated after rectal administration of three different contrast agents, including tap water, diluted barium, or air, on ultrasonography in healthy dogs, the thickness of the colonic wall was highest after the administration of water, followed by barium and air [37]. In addition, hydrosonography using water alone allows visualization of the mucosal and muscular layers of the colon [37]. Similarly, in humans, the infusion of saline decreased the concentration of fecal residues and improved the clarity of the colonic wall [38]. In 17 children, GI hydrosonography of the colon using saline allowed evaluation of the entire colon and detection of colorectal polyps [38]. Moreover, the administration of warm tap water into the rectum can increase the diagnostic accuracy of pelvic masses and delineate the extent of tumors arising from intrapelvic organs such as the bladder, prostate, and uterus by improving the acoustic window in human patients [33].

Saline infusion is commonly used in sono-urethrography in humans [39, 40]. Sono-urethrography can show various imaging features and has several strengths depending on the UCA used [28]. In healthy dogs, agitated saline and SonoVue showed hyperechoic signals created by bubbles, which were useful for the identification of the urethra compared to anechoic saline [28]. Sono-urethrography using saline or agitated saline infusion could improve the visualization of the urethral wall and lumen because it does not induce significant shadowing artifacts, which can impair the urinary tract image quality. In our study, sono-urethrography was performed using agitated saline in all 4 cases because we expected that the hyperechoic signals generated from the bubbles would improve urine flow in dogs with urinary tract abnormalities. The hyperechoic bubbles could be formed easily in agitated saline, allowing visualization of the urethral lumen and communication between the prostatic cysts because the saline bubbles showed hyperechoic signals in contrast with the hypoechoic fluid in the cyst and urethral lumen. Moreover, agitated saline clearly showed the normally dilated lumen of the prostatic urethra and excluded narrowing or obstruction of the urethra by the enlarged prostatic lobe in dogs with pyogranulomatous prostitis. Similarly, sono-urethrography using saline or UCAs has been used to detect anterior urethral strictures and to clarify their location and length in human patients [39, 40].

Microbubbles in agitated saline and UCAs can improve image quality by absorbing, attenuating, and scattering ultrasound signals more than the surrounding tissue and subsequently enhancing the image contrast of microbubbles from the surrounding tissues [41, 42]. However, our study found that sono-urethrography using agitated saline was limited in detecting and localizing bladder rupture, and required additional sono-urethrography using SonoVue. The use of SonoVue in sono-urethrography generated a stronger and brighter signal of microbubbles than agitated saline. This allowed us to successfully demonstrate leakage from small ruptured areas of the bladder into the peritoneal space. A previous study involving healthy dogs indicated the potential of sono-urethrography using UCA to assess urethral integrity, and this was supported by improved conspicuity of the urethra when using UCAs as opposed to saline or agitated saline [28]. This result could be related to the different characteristics of the microbubbles in agitated saline and UCAs, such as size, gas composition, solubility of air in the fluid, and stability [41, 43]. Microbubbles in the agitated saline are generally considered >10 micrometers in diameter and larger than the microbubbles in UCAs at approximately 1-10 micrometer diameters [43]. Microbubbles in agitated saline are unstable and rapidly dissolve because of their high solubility compared to UCA microbubbles, which contain fluorinated gases, such as sulfur hexafluoride, and are stabilized by phospholipids and other amphiphilic polymeric shells [43]. Therefore, the UCA induced a strong and uniform signal that was strong enough for the detection of hyperechoic microbubbles leaked from small defects in the urinary tract.

Although saline infusion was not used to evaluate the urinary tract in our study, its use in sono-urethrography should be limited to dogs with urinary diseases because of the short duration of the

examination with saline infusion in healthy dogs [28]. Considering the need to scrutinize the entire urethra in patients, continuous infusion of saline may be required to prevent urethral collapse that can occur after the completion of saline infusion.

In this study, sono-urethrography was applied to our cases as an alternative to traditional radiographic contrast studies such as retrograde urethrography and voiding cystourethrography, which are commonly used in veterinary medicine to evaluate the diameter, wall, lumen, and integrity of the urethra [44]. The reason for this choice was the limited capability of radiographic urethrography in detecting subtle mucosal changes within the urethra. Additionally, sono-urethrography could be easily performed on the lower urinary tract without need of anesthesia. This technique provides real-time imaging of the intraabdominal urethra in females and the prostatic as well as penile urethra in male dogs and facilitates repeated examinations until the lesion's features are clearly assessed [40, 45].

This study had several limitations. First, intraluminal CEUS was performed only as GI hydrosonography and sono-urethrography because this study was performed in patients with naturally developed conditions. Second, sonographic examination of urinary conditions was conducted in only a small number of patients. Further studies on the application of this technique in various urinary tract conditions, including tumors, inflammation, and strictures, which can induce narrowing or obstruction of the urethral lumen, filling defects, thickening, and irregularity of the mucosa, are needed in dogs and cats.

## 4. Conclusions

In conclusion, intraluminal CEUS examinations were performed using various UCAs in patients with GI and urinary diseases. Intraluminal CEUS examinations helped to assess the patency of the lumen, evaluate the extent of luminal dilation, rule out luminal narrowing, determine the presence of a mass within the lumen, and identify rupture sites. Intraluminal CEUS using saline or agitated saline is appropriate for filling the lumen and improving the acoustic window for GI hydrosonography. Intraluminal CEUS with agitated saline and SonoVue is useful for assessing abnormal connections and detecting ruptures. Intraluminal CEUS using SonoVue, water, agitated saline, and saline is useful and easily performed to evaluate the GI tract, lower urinary tract, and prostate in dogs and cats without the need for anesthesia.

**Institutional Review Board Statement:** The requirement of ethical approval was waived by Chonnan National University for Research Ethics for the studies involving animals because this study is a case report, and only retrospective information about the patient was utilized. No separate experiments or sampling were conducted for the purpose of this report. The studies were conducted in accordance with the local legislation and institutional requirements. Written informed consent was obtained from the owners for the participation of their animals in this study.

**Informed Consent Statement:** Informed consent was obtained from owner.

**Data Availability Statement:** Not applicable.

**Conflicts of Interest:** The authors declare no conflict of interest.

## References

1.  Caine A, Agthe P, Posch B, Herrtage M. Sonography of the soft tissue structures of the canine tarsus. Vet Radiol Ultrasound. 2009, 50, 304–308.
2.  Valls Sanchez F, Puig J, Olivares G, Holloway A, Seth M. Association between ultrasonographic appearance of urine and urinalysis in dogs and cats. JSAP. 2019, 60, 361–366.
3.  Nyman HT, Nielsen OL, McEvoy FJ, Lee MH, Martinussen T, Hellmén E, et al. Comparison of B-mode and Doppler ultrasonographic findings with histologic features of benign and malignant mammary tumors in dogs. Am J Vet Res. 2006, 67, 985–991.
4.  Baier J, Rix A, Kiessling F. Molecular Ultrasound Imaging. Recent Results Cancer Res. 2020, 216, 509-531
5.  Badea R, Ciobanu L, Gomotirceanu A, Hagiu C, Socaciu M. Contrast ultrasonography of the digestive tract lumen. Review of the literature and personal experience. Med Ultrason. 2010, 12, 52–61.
6.  Zvanca M, Andrei C. Volume Ultrasound in Uterine and Tubal Evaluation. DJSUOG. 2011, 5, 243–256.
7.  Klibanov AL. Ultrasound Contrast. Invest Radiol. 2021, 56, 50–61.
8.  Gharat SK, Godiyal SC, Malusare PP, Jadhav KR, Kadam VJ. Microbubbles Contrast Agents: General Overview as Diagnostics and Therapeutic Agent. Curr Drug Targets. 2022, 23, 960–977.
9.  Baron Toaldo M, Diana A, Bettini G, Di Donato P, Linta N, Cipone M. Imaging diagnosis-cholangiocellular adenoma: contrast-enhanced ultrasonographic findings of a benign tumor mimicking malignant neoplasia in a dog. Vet Radiol Ultrasound. 2013, 54, 71–74.
10. Nyman HT, Kristensen AT, Kjelgaard-Hansen M, McEvoy FJ. Contrast-enhanced ultrasonography in normal canine liver. Evaluation of imaging and safety parameters. Vet Radial Ultrasound. 2005, 46, 243–250.
11. Ohlerth S, Dennler M, Rüefli E, Hauser B, Poirier V, Siebeck N, et al. Contrast Harmonic Imaging Characterization of Canine Splenic Lesions. J Vet Intern Med. 2008, 22, 1095–1102.
12. Weber MA, Krakowski-Roosen H, Hildebrandt W, Schröder L, Ionescu I, Krix M, Kinscherf R, Bachert P, Kauczor HU, Essig M. Assessment of metabolism and microcirculation of healthy skeletal muscles by magnetic resonance and ultrasound techniques. J Neuroimaging. 2007, 17, 323-331.
13. Pey P, Daminet S, Smets PMY, Duchateau L, De Fornel-Thibaud P, Rosenberg D, et al. Contrast-enhanced ultrasonographic evaluation of adrenal glands in dogs with pituitary-dependent hyperadrenocorticism. Am J Vet Res. 2013, 74, 417–425.
14. Pey P, Vignoli M, Haers H, Duchateau L, Rossi F, Saunders JH. Contrast-enhanced ultrasonography of the normal canine adrenal gland. Vet Radiol Ultrasound. 2011, 52, 560–567.
15. Rademacher N, Ohlerth S, Scharf G, Laluhova D, Sieber-Ruckstuhl N, Alt M, et al. Contrast-Enhanced Power and Color Doppler Ultrasonography of the Pancreas in Healthy and Diseased Cats. J Vet Intern Med. 2008, 22, 1310–1316.
16. Johnson-Neitman JL, O'Brien RT, Wallace JD. Quantitative perfusion analysis of the pancreas and duodenum in healthy dogs by use of contrast-enhanced ultrasonography. Am J Vet Res. 2012, 73, 385–392.
17. Haers H, Daminet S, Smets PMY, Duchateau L, Aresu L, Saunders JH. Use of quantitative contrast-enhanced ultrasonography to detect diffuse renal changes in Beagles with iatrogenic hypercortisolism. Am J Vet Res. 2013, 74, 70–77.
18. Cordella A, Pey P, Linta N, Quinci M, Baron Toaldo M, Pisoni L, et al. Use of Contrast-Enhanced Ultrasonography for the Characterization of Tumor Thrombi in Seven Dogs. Animals. 2020, 10, 1613.
19. Claudon M, Dietrich CF, Choi BI, Cosgrove DO, Kudo M, Nolsøe CP, et al. Guidelines and Good Clinical Practice Recommendations for Contrast Enhanced Ultrasound (CEUS) in the Liver – Update 2012. Ultrasound Med Biol. 2013, 39, 187–210.
20. Nolsøe CP, Nolsøe AB, Klubien J, Pommergaard H-C, Rosenberg J, Meloni MF, et al. Use of Ultrasound Contrast Agents in Relation to Percutaneous Interventional Procedures: A Systematic Review and Pictorial Essay. JUM. 2018, 37, 1305–1324.
21. Lorentzen T, Nolsøe CP, Ewertsen C, Nielsen MB, Leen E, Havre RF, Gritzmann N, Brkljacic B, Nürnberg D, Kabaalioglu A, Strobel D, Jenssen C, Piscaglia F, Gilja OH, Sidhu PS, Dietrich CF; EFSUMB. EFSUMB Guidelines on Interventional Ultrasound (INVUS), Part I. General Aspects. Ultraschall Med. 2015, 36, E1-14.
22. Sparchez Z, Mocan T, Hagiu C, Kacso G, Zaharie T, Rusu I, et al. Real-Time Contrast-Enhanced–Guided Biopsy Compared with Conventional Ultrasound–Guided Biopsy in the Diagnosis of Hepatic Tumors on a Background of Advanced Chronic Liver Disease: A Prospective, Randomized, Clinical Trial. Ultrasound Med Biol. 2019, 45, 2915–2924.

23. Francica G. Intracavitary contrast-enhanced ultrasound in ultrasound-guided percutaneous management of abdominal fluid collections/abscesses by a single clinician: an example of point-of-care ultrasound. J Ultrasound. 2020, 23, 175–181.

24. Xu E-J, Zhang M, Li K, Su Z-Z, Long Y-L, Zeng Q-J, et al. Intracavitary Contrast-Enhanced Ultrasound in the Management of Post-Surgical Gastrointestinal Fistulas. Ultrasound Med Biol. 2018, 44, 502–507.

25. Deganello A, Rafailidis V, Sellars ME, Ntoulia A, Kalogerakou K, Ruiz G, et al. Intravenous and Intracavitary Use of Contrast-Enhanced Ultrasound in the Evaluation and Management of Complicated Pediatric Pneumonia. JUM. 2017, 36, 1943–1954.

26. Pei F, Liu Y, Zhang F, Li N, Huang D, Gu B. Cholecystoduodenal fistula: ultrasonographic diagnosis with oral gastrointestinal ultrasound contrast medium. Abdom Imaging. 2011, 36, 561–564.

27. Sudoł-Szopińska I, Jakubowski W, Szczepkowski M. Contrast-enhanced endosonography for the diagnosis of anal and anovaginal fistulas. J Clin Ultrasound. 2002, 30, 145-150.

28. Park S, Jung J-W, Jang S, Choi B-K, Lee E, Lee S, et al. Efficacy of a phospholipid-stabilized sulfur hexafluoride microsphere contrast agent and water for hydrosonography of the upper portion of the gastrointestinal tract in dogs. Am J Vet Res. 2021, 82, 712–721.

29. Lee D, Yoon S, Kim C, Choi J. A comparative study of sono-urethrography using saline, agitated saline, and an ultrasound contrast agent in normal beagles. Vet Radiol Ultrasound. 2021, 62, 342–349.

30. Trikoupi G, Papadopoulou P, Papadopoulou F, Theodoridis A, Papazoglou L, Patsikas M. Contrast-enhanced voiding urosonography: A new, radiation-free, alternative method for imaging of urinary bladder and urethra in healthy dogs. Vet Radiol Ultrasound. 2020, 61, 453–460.

31. Muehlbauer E, Saldanha A, Gil EM, Alves TL, Duque JCM, Froes TR. The use of agitated saline as contrast agent in a contrast-enhanced cystosonography for detection of urinary bladder rupture in animal cadavers. J Vet Emerg Crit Care (San Antonio). 2023, 33, 327-331.

32. Maconi G, Radice E, Bareggi E, Porro GB. Hydrosonography of the Gastrointestinal Tract. Am J Roentgenol. 2009, 193, 700–708.

33. Rubin C, Kurtz AB, Goldberg BB. Water enema: a new ultrasound technique in defining pelvic anatomy. J Clin Ultrasound. 1978, 6,28-33.

34. Suciu MD, Marica NA, Badea AF, Gavrila IL, Badea RI. Retrograde urethrosonography with SonoVue in strictures of the male urethra: a pilot study. Med Ultrason. 2020, 22, 424

35. Ishigami K, Abu-Yousef DM, Kao SC, Abu-Yousef MM. Comparison of 2 oral ultrasonography contrast agents: simethicone-coated cellulose and simethicone-water rotation in improving pancreatic visualization. Ultrasound Q. 2014, 30, 135-138.

36. Ravikumar BR, Tejus C, Madappa KM, Prashant D, Dhayanand GS. A comparative study of ascending urethrogram and sono-urethrogram in the evaluation of stricture urethra. International Braz j Urol. 2015, 41, 388–392.

37. Cheon B, Moon S, Park S, Lee SK, Hong S, Cho H, Choi J. Comparison of contrast media for visualization of the colon of healthy dogs during computed tomography and ultrasonography. Am J Vet Res. 2016, 77, 1220-1226.

38. Ling UP, Chen JY, Hwang CJ, Lin CK, Chang MH. Hydrosonography in the evaluation of colorectal polyps. Arch Dis Child. 1995, 73, 70–73.

39. Ani C, Akpayak I, Dakum N, Ramyil V, Shuaibu S. Sonourethrography in the evaluation of anterior urethral stricture. J West Afr Coll Surg. 2012, 2, 1–13.

40. B.R. R, Tejus C, K.M. M, Prashant D, G.S. D. A comparative study of ascending urethrogram and sono-urethrogram in the evaluation of stricture urethra. International Braz j Urol. 2015, 41, 388–392.

41. Cosgrove D. Ultrasound contrast agents: an overview. Eur J Radiol. 2006, 60, 324-30.

42. Cosgrove D, Harvey C. Clinical uses of microbubbles in diagnosis and treatment. Med Biol Eng Comput. 2009, 47, 813-26.Seerla DrVN, Vedaraju DrK, Baru DrRR, Suneetha DrP, B DrA, Saikrishna DrMT, et al. Study of sonourethrography in comparision to conventional retrograde urethrography in evaluation of male urethral pathologies. IJRDI. 2021, 4, 15–29.

43. Koo B, Liu Y, Abboud M, Qin B, Wu Y, Choi S, Kozak D, Zheng J. Characterizing how size distribution and concentration affect echogenicity of ultrasound contrast agents. Ultrasonics. 2023, 127, 106827.

44. Darge K, Troeger J, Deutting T, Zieger B, Rohrschneider W, Moehring K, Weber C, Toenshoff B. Reflux in young patients: comparison of voiding US of the bladder and retrovesical space with echo enhancement versus voiding cystourethrography for diagnosis. Radiology. 1999, 210, 201-207.

45. Morey AL, McAninch JW. Ultrasound evaluation of the male urethra for assessment of urethral stricture. J Clin Ultrasound. 1996, 24, 473-479.